

# A Study on the Accurate Equation Inversion Method for Uncoupled Interface Parameters of OA Media Considering Initial Stress

Zihang Fan<sup>1, a</sup>, Zhaoyun Zong<sup>1, b \*</sup>

<sup>1</sup> School of Earth Sciences and Technology, China University of Petroleum (East China), Qingdao Shandong, China.

<sup>a</sup>zihang\_fan@163.com, <sup>b</sup>zongzhaoyun@upc.edu.cn

**Abstract.** Underground media are generally affected by the initial stress of the overlying strata. At the same time, the uncoupled interface is an important influencing factor of seismic response, as well as an essential reservoir environment, reservoir space, and migration channel. It is significant to explore the parameters of the uncoupled interface under stress for identifying oil and gas reservoirs. As an effective means of predicting reservoir physical parameters, pre-stack seismic inversion uses information on uncoupled interface fractures under stress to improve the accuracy of reservoir parameter prediction, overcome the problem of insufficient interface parameter prediction methods, and promote oil and gas reservoir exploration and development. Based on the precise equations for directly characterizing uncoupled interface fracture weakness parameters, this paper uses the ANNI inversion method to realize the nonlinear inversion method of uncoupled interface fracture parameters. The feasibility and practicability of predicting underground medium parameters from seismic response characteristics have been verified through model testing and actual work area application.

**Keywords:** OA media; Initial Stress Induce; Nonlinear Inversion; ANNI Inversion.

## 1. Introduction

Underground fractures and reservoirs are generally affected by initial stress from surrounding rocks and overlying strata, which usually affects the medium's wave propagation characteristics and elastic properties [1-3], The acoustoelastic theory is generally used for reasonable description and explanation in the research process. The acoustoelastic effect refers to the change of sound velocity (longitudinal wave and transverse wave velocity) in elastic materials under the action of the initial static stress field. Acoustoelasticity theory is also known as third-order nonlinear elasticity theory. It assumes that the strain energy includes the quadratic and cubic terms in the classical elasticity theory. At the same time, the theory can also be summarized by the nonlinear constitutive relationship between mechanical stress and effective strain in continuous medium materials.

The uncoupled interface, also called the discontinuous interface, generally refers to discontinuous interfaces such as cracks, faults, joints, and unconformities. This interface is widely distributed in the earth's interior and impacts the storage and migration of oil and gas. Linear slip theory is currently the most important basic theory to describe uncoupled interfaces [4, 5], This theory uses fracture weakness terms to describe cracks, ignores the shape and structure of the cracks, and assumes the cracks to be a plane with no thickness. At the same time, linear slip theory can also guide the boundary conditions of the uncoupled interface. According to the theoretical assumption, the boundary conditions of the uncoupled interface are stress continuity, and the displacement difference is equal to the product of stress and fracture weakness.

In pre-stack seismic inversion, although the approximate equations [6-7] and the exact equations [8] give approximately the same results under the assumptions of weak anisotropy and small incident angles, this assumption does not always hold [9]. The inversion results will produce significant errors when the interlayer medium changes significantly. In this case, the results of the approximate equations will need to be more accurate and stable, which prompted the introduction of nonlinear inversion methods into the field of geophysics. With the development of technology, artificial intelligence has allowed geophysicists to see new inversion tools. By combining the

precise Zoeppritz equation with the Artificial Neural Network Inversion Tool (ANNI), it is possible to estimate and predict the six parameters in the equation. At the same time, a new form of the exact Zoeppritz equation was derived using methods such as Taylor expansion to reduce the difficulty of inversion [10-13]. With the development of pre-stack nonlinear inversion methods in anisotropic media, the MCMC (Markov Chain Monte Carlo) algorithm is used to directly perform AVO accurate inversion, providing a reference for nonlinear inversion of anisotropic media [13]. For VTI media, an exact equation inversion method based on isotropic reflection coefficients and linear approximate anisotropic terms was developed [14] to overcome the anisotropy assumption in theory.

At present, scholars have developed a variety of seismic inversion methods based on precise equations for different media. However, more consideration is needed of the actual situation of initial stress and the uncoupled interface. It is urgent to explore the inversion method of complex anisotropic medium reservoir parameters based on precise equations considering the effect of initial stress and to verify the rationality of inverting complex medium reservoir parameters from precise seismic responses.

## 2. An accurate equation inversion method for uncoupled interface parameters based on ANNI

Discontinuous uncoupled interfaces such as cracks and faults are commonly developed in actual underground reservoirs and are essential storage spaces and migration pathways for oil and gas. Based on the reflection and transmission coefficient equation of the uncoupled interface of orthogonal anisotropic media under initial stress, an exact equation forward operator is constructed. By utilizing the precise characteristics of the exact equation and combining it with the ANNI inversion method, research on the exact equation inversion method for uncoupled interface fracture weakness is conducted, which is beneficial to understanding the state of underground horizontal fractures and improving the exploration and development efficiency and prediction accuracy of shale reservoirs.

### 2.1 Construction of reflection coefficient equation under initial stress

The equivalent stiffness matrix is the most important parameter for constructing the stress-strain relationship. Substitute the elastic parameters of the OA medium without stress in the background medium into the equivalent elastic parameter expression based on the acoustoelastic theory. The equivalent stiffness coefficient matrix [15] can be simplified to:

$$C_{ijkl} = c_{ijkl} + c_{ijklmn} E_{mn} \quad (1)$$

Where  $C_{ijkl}$  is the equivalent stiffness matrix of the OA medium after the initial stress, and  $c_{ijkl}$  and  $c_{ijklmn}$  are the second-order and third-order elastic tensors of the OA medium without stress in the background medium. According to the symmetry assumption, the third-order elastic parameter of the OA medium is  $c_{111}, c_{112}, c_{123}, c_{113}, c_{133}, c_{144}, c_{155}, c_{222}, c_{333}, c_{344}$ . According to the expression of equation (1), the equivalent stiffness coefficient of the OA medium under the initial stress can be obtained:

$$\begin{aligned} C_{11} &= c_{11} + c_{111}E_{11} + c_{112}E_{22} + c_{113}E_{33}; C_{12} = c_{12} + c_{111}E_{11} + c_{112}E_{22} + c_{113}E_{33}; \\ C_{13} &= c_{13} + c_{113}E_{11} + c_{123}E_{22} + c_{133}E_{33}; C_{22} = c_{22} + (c_{111} + c_{112} - c_{222})E_{11} + c_{222}E_{22} + c_{113}E_{33}; \\ C_{23} &= c_{23} + c_{123}E_{11} + c_{113}E_{22} + c_{133}E_{33}; C_{33} = c_{33} + c_{133}E_{11} + c_{133}E_{22} + c_{333}E_{33}; \\ C_{44} &= c_{44} + c_{144}E_{11} + c_{155}E_{22} + c_{344}E_{33}; \quad C_{55} = c_{55} + c_{155}E_{11} + c_{144}E_{22} + c_{344}E_{33}; \quad (2) \\ C_{66} &= c_{66} + \frac{-2c_{111} - c_{112} + 3c_{222}}{4}E_{11} + \frac{2c_{111} - c_{112} - c_{222}}{4}E_{22} + \frac{c_{113} - c_{123}}{2}E_{33} \\ C_{21} &= C_{12}; C_{32} = C_{23}; C_{31} = C_{13}; \end{aligned}$$

$E_{mn}$  is the strain tensor, represented by  $T_{ij} = c_{ijkl}E_{kl}$ , and  $T_{ij}$  is the vertical initial stress. The above parameter subscripts all use the Voigt notation method, specifically 11→1, 22→2, 33→3, 32 or 23→4, 31 or 13→5, 21 or 12→6.

In order to obtain the accurate reflection coefficient of the uncoupled interface of OA medium under stress, it is assumed that the front of the seismic wave is planes and incident at a fixed angle.

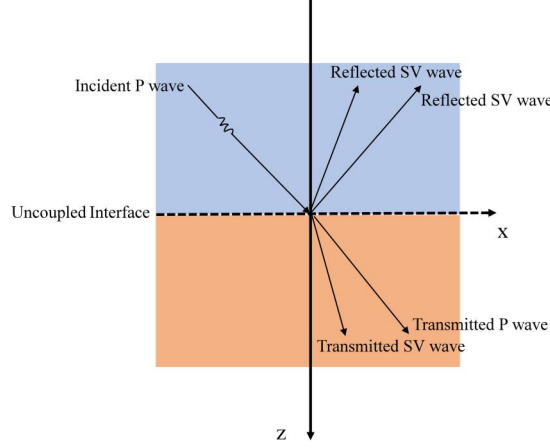


Fig. 1 Plane P-wave incidence diagram

The model is shown in Fig. 1. The upper medium is isotropic, and the lower medium is OA medium. The vertical direction along the z-axis is defined as the positive direction. P wave incidence will generate four types of waves, and  $\theta_{ip}, \theta_{rp}, \theta_{rs}, \theta_{tp}, \theta_{ts}$  represents the incident angles of the incident P wave, reflected P, reflected SV wave, transmitted P, and transmitted SV wave, respectively.

According to the acoustoelastic theory, the stress term in the boundary condition can be expressed as:

$$T_{ij} = C_{ijkl}e_{kl} + u_{i,k}\tau_{kj} \quad (3)$$

Where  $T_{ij}$  is stress on both sides of the interface,  $C_{ijkl}$  is the equivalent stiffness coefficient matrix under stress,  $e_{kl}$  is strain, which can be expressed as  $(u_{k,l} + u_{l,k})$ , the subscript comma represents the derivative, and  $\tau_{kj}$  represents the initial stress. This section assumes the initial stress only considers the vertical downward stress, i.e.  $\tau = (0,0,\tau_{33},0,0,0)$ . Where  $u_i$  is the plane wave displacement, expressed explicitly as:

$$u_i^R = A^R P_i^R \exp[i\omega(s_j^R X_j) - t] \quad (4)$$

$i$  represents the imaginary term,  $\omega$  represents the angular frequency,  $P_i^R$  represents the polarization vector,  $s_j^R$  represents the slowness vector,  $t$  represents the time, the superscript  $R = (0,1,2,\dots,4)$  represents the type of wave, and the subscript represents the component of the polarization vector.

In this paper, for the uncoupled interface, based on Schoenberg linear slip theory, it is assumed that the boundary conditions are stress continuity, displacement discontinuity, and the displacement difference between the upper and lower media is linearly correlated with the stress. Specifically, it can be expressed as:

$$\begin{aligned} \Delta u &= ZT; \\ (T_{3i})^{up} &= (T_{3i})^{low} \quad i=1,3 \end{aligned} \quad (5)$$

Equation (5) can be expanded in two dimensions as follows:

$$\begin{aligned}
\left( \sum_{R=3}^4 u_1^R - \sum_{R=0}^2 u_1^R \right) &= \left[ \sum_{R=0}^2 \Delta_T T_{31}^R \right] \\
\left( \sum_{R=3}^4 u_3^R - \sum_{R=0}^2 u_3^R \right) &= \left[ \sum_{R=0}^2 \Delta_N T_{33}^R \right] \\
\left( \sum_{R=3}^4 T_{33}^R \right) &= \left( \sum_{R=0}^2 T_{33}^R \right) \\
\left( \sum_{R=3}^4 T_{31}^R \right) &= \left( \sum_{R=0}^2 T_{31}^R \right)
\end{aligned} \tag{6}$$

Where  $\Delta_N$ ,  $\Delta_T$  is the normal and tangential fracture parameters respectively, expand (6) and organize them into a matrix form:

$$\begin{aligned}
GR &= M \\
G &= \begin{bmatrix} \mathcal{G}_{11} & \mathcal{G}_{12} & \mathcal{G}_{13} & \mathcal{G}_{14} \\ \mathcal{G}_{21} & \mathcal{G}_{22} & \mathcal{G}_{23} & \mathcal{G}_{24} \\ \mathcal{G}_{31} & \mathcal{G}_{32} & \mathcal{G}_{33} & \mathcal{G}_{34} \\ \mathcal{G}_{41} & \mathcal{G}_{42} & \mathcal{G}_{43} & \mathcal{G}_{44} \end{bmatrix}; \\
R &= [R_{PP} \quad R_{PS} \quad T_{PP} \quad T_{PS}]; \\
M &= [m_1 \quad m_2 \quad m_3 \quad m_4]
\end{aligned} \tag{7}$$

The specific representation of the elements in the matrix is:

$$\begin{aligned}
\mathcal{G}_{11} &= -\left( P_{rp1} + i\omega\Delta_T (Ca_{55}(P_{rp1}s_3^1 + P_{rp3}s_1^1)) \right); \mathcal{G}_{12} = -\left( P_{rs1} + i\omega\Delta_T (Ca_{55}(P_{rs1}s_3^1 + P_{rs3}s_1^1)) \right); \\
\mathcal{G}_{13} &= P_{ip1}; \quad \mathcal{G}_{14} = P_{is1}; \\
\mathcal{G}_{21} &= -\left( P_{rp3} + i\omega\Delta_N (Ca_{31}P_{rp1}s_1^1 + Ca_{33}P_{rp3}s_3^1 + P_{rp3}s_3^1T_{33}) \right); \\
\mathcal{G}_{22} &= -\left( P_{rs3} + i\omega\Delta_N (Ca_{31}P_{rs1}s_1^2 + Ca_{33}P_{rs3}s_3^2 + P_{rs3}s_3^2T_{33}) \right); \\
\mathcal{G}_{23} &= P_{ip3}; \quad \mathcal{G}_{24} = P_{is3}; \\
\mathcal{G}_{31} &= Ca_{55}(P_{rp1}s_3^1 + P_{rp3}s_1^1); \mathcal{G}_{32} = Ca_{55}(P_{rs1}s_3^2 + P_{rs3}s_1^2); \\
\mathcal{G}_{33} &= -Cb_{55}(P_{ip3}s_1^3 + P_{ip1}s_3^3); \mathcal{G}_{34} = -Cb_{55}(P_{is3}s_1^4 + P_{is1}s_3^4); \\
\mathcal{G}_{41} &= Ca_{31}P_{rp1}s_1^1 + Ca_{33}P_{rp3}s_3^1 + P_{rp3}s_3^1T_{33}; \mathcal{G}_{42} = Ca_{31}P_{rs1}s_1^2 + Ca_{33}P_{rs3}s_3^2 + P_{rs3}s_3^2T_{33}; \\
\mathcal{G}_{43} &= -(Cb_{31}P_{ip1}s_1^3 + Cb_{33}P_{ip3}s_3^3 + P_{ip3}s_3^3T_{33}); \mathcal{G}_{44} = -(Cb_{31}P_{is1}s_1^4 + Cb_{33}P_{is3}s_3^4 + P_{is3}s_3^4T_{33}); \\
m_1 &= -\left( P_{ip1} + i\omega\Delta_T (Ca_{55}(P_{ip1}s_3^0 + P_{ip3}s_1^0)) \right); m_2 = -\left( P_{ip3} + i\omega\Delta_N (Ca_{31}P_{ip1}s_1^0 + Ca_{33}P_{ip3}s_3^0 + P_{ip3}s_3^0T_{33}) \right); \\
m_3 &= Ca_{55}(P_{ip1}s_3^0 + P_{ip3}s_1^0); m_4 = Ca_{31}P_{ip1}s_1^0 + Ca_{33}P_{ip3}s_3^0 + P_{ip3}s_3^0T_{33}
\end{aligned} \tag{8}$$

Where  $Ca_{ij}$  represents the elastic parameter of the upper medium,  $Cb_{ij}$  represents the elastic parameter of the lower medium,  $P_{ip}$ ,  $P_{rp}$ ,  $P_{rs}$ ,  $P_{tp}$ ,  $P_{ts}$  are the polarization directions of the incident P wave, reflected P, S wave, and transmitted P, S wave, respectively. The superscripts 0 to 4 correspond to the incident P wave, reflected P, S wave, and transmitted P, S wave, respectively. Subscripts 1 and 3 correspond to the components in the two directions. Finally, the matrix inversion is used to obtain the accurate reflection and transmission coefficients:

$$R = L^{-1}M \tag{9}$$

## 2.2 Inversion of the exact equations of the uncoupled interface parameters under initial stress

Since the exact PP wave reflection coefficient solved by the exact equation is an explicit expression expressed by parameters, it would be very complicated to solve it directly. At the same

time, it can be found through observation that the fracture weakness of the uncoupled interface of the inversion parameter is not included in the medium-related parameters such as stiffness coefficient, polarization or slowness, so it is assumed that:

$$\begin{aligned}
X_{a0} &= Ca_{55}(P_{ip1}s_3^0 + P_{ip3}s_1^0); & X_{a1} &= Ca_{55}(P_{rp1}s_3^1 + P_{rp3}s_1^1); & X_{a2} &= Ca_{55}(P_{rs1}s_3^1 + P_{rs3}s_1^1); \\
X_{b3} &= Cb_{55}(P_{ip3}s_1^3 + P_{ip1}s_3^3); & X_{b4} &= Cb_{55}(P_{is3}s_1^4 + P_{is1}s_3^4); \\
Y_{a0} &= Ca_{31}P_{ip1}s_1^0 + Ca_{33}P_{ip3}s_3^0 + P_{ip3}s_3^0T_{33}; & Y_{a1} &= Ca_{31}P_{rp1}s_1^1 + Ca_{33}P_{rp3}s_3^1 + P_{rp3}s_3^1T_{33}; \\
Y_{a2} &= Ca_{31}P_{rs1}s_1^2 + Ca_{33}P_{rs3}s_3^2 + P_{rs3}s_3^2T_{33}; & Y_{b3} &= Cb_{31}P_{ip1}s_1^3 + Cb_{33}P_{ip3}s_3^3 + P_{ip3}s_3^3T_{33}; \\
Y_{b4} &= Cb_{31}P_{is1}s_1^4 + Cb_{33}P_{is3}s_3^4 + P_{is3}s_3^4T_{33}
\end{aligned} \tag{10}$$

According to the new assumption, G and M in the matrix (8) can be simplified to:

$$\begin{aligned}
g_{11} &= -(P_{rp1} + i\omega\Delta_T X_{a1}); & g_{12} &= -(P_{rs1} + i\omega\Delta_T X_{a2}); & g_{21} &= -(P_{rp3} + i\omega\Delta_N Y_{a1}); & g_{22} &= -(P_{rs3} + i\omega\Delta_N Y_{a2}); \\
g_{23} &= P_{ip3}; & g_{24} &= P_{is3}; & g_{13} &= P_{ip1}; & g_{14} &= P_{is1}; & g_{31} &= X_{a1}; & g_{32} &= X_{a2}; \\
g_{33} &= -X_{b3}; & g_{34} &= -X_{b4}; & g_{41} &= Y_{a1}; & g_{42} &= Y_{a2}; & g_{43} &= -Y_{b3}; & g_{44} &= -Y_{b4}; \\
m_1 &= -(P_{ip1} + i\omega\Delta_T X_{a0}); & m_2 &= -(P_{ip3} + i\omega\Delta_T Y_{a0}); & m_3 &= -X_{a0}; & m_4 &= -Y_{a0};
\end{aligned} \tag{11}$$

By solving the above equation, we can obtain the solution of the exact equation of the uncoupled interface PP wave reflection coefficient under the action of initial stress.

$$R_{PP} = \frac{-a_1 b_1 + c_1 d_1}{a_2 b_2 - c_2 d_2}, a_2 = a_1, d_2 = d_1 \tag{12}$$

Where:

$$\begin{aligned}
a_1 &= -m_1 n_1 + P_{is3} X_{a2} n_4 - P_{rs3} X_{b4} n_4 - i\omega X_{b4} Y_{a2} n_4 \Delta_N; & b_1 &= m_2 n_2 - P_{is1} X_{a0} n_4 - P_{ip1} X_{b4} n_4 - i\omega X_{a0} Y_{b4} n_4 \Delta_T; \\
c_1 &= m_1 n_2 - P_{is3} X_{a0} n_4 - P_{ip3} X_{b4} n_4 - i\omega X_{b4} Y_{a0} n_4 \Delta_N; & d_1 &= m_2 n_1 - P_{is1} X_{a2} n_4 + P_{rs1} X_{b4} n_4 + i\omega X_{a2} Y_{b4} n_4 \Delta_T; \\
b_2 &= m_2 n_3 - P_{is1} X_{a1} n_4 + P_{rp1} X_{b4} n_4 + i\omega X_{a1} Y_{b4} n_4 \Delta_T; & c_2 &= m_1 n_3 - P_{is3} X_{a1} n_4 + P_{rp3} X_{b4} n_4 + i\omega X_{b4} Y_{a1} n_4 \Delta_N; \\
m_1 &= -P_{is3} X_{b3} + P_{ip3} X_{b4}; & m_2 &= -P_{is1} X_{b3} + P_{ip1} X_{b4}; \\
n_1 &= -X_{b4} Y_{a2} + X_{a2} Y_{b4}; & n_2 &= -X_{b4} Y_{a0} + X_{a0} Y_{b4}; \\
n_3 &= -X_{b4} Y_{a1} + X_{a1} Y_{b4}; & n_4 &= X_{b4} Y_{b3} - X_{b3} Y_{b4}
\end{aligned} \tag{13}$$

The PP wave reflection coefficient of a two-dimensional uncoupled interface is expressed as:

$$R_{pp} = - \frac{\left( \begin{aligned} & \left( - \left( P_{is3} X_{b3} - P_{ip3} X_{b4} \right) \left( - X_{b4} Y_{a2} + X_{a2} Y_{b4} \right) + \left( X_{b4} Y_{b3} - X_{b3} Y_{b4} \right) \left( P_{rs3} X_{a2} - X_{b4} \left( P_{rs3} - i \omega \Delta_N \right) \right) \right) \\ & \left( - \left( P_{is1} X_{b3} - P_{ip1} X_{b4} \right) \left( - X_{b4} Y_{a0} + X_{a0} Y_{b4} \right) + \left( X_{b4} Y_{b3} - X_{b3} Y_{b4} \right) \left( P_{rs1} X_{a0} - X_{b4} \left( P_{rs1} + i \omega \Delta_N \right) \right) \right) \\ & + \left( - \left( P_{is3} X_{b3} - P_{ip3} X_{b4} \right) \left( - X_{b4} Y_{a0} + X_{a0} Y_{b4} \right) + \left( X_{b4} Y_{b3} - X_{b3} Y_{b4} \right) \left( P_{rs3} X_{a0} - X_{b4} \left( P_{ip3} + i \omega \Delta_N \right) \right) \right) \\ & \left( - \left( P_{is1} X_{b3} - P_{ip1} X_{b4} \right) \left( - X_{b4} Y_{a2} + X_{a2} Y_{b4} \right) + \left( X_{b4} Y_{b3} - X_{b3} Y_{b4} \right) \left( P_{rs1} X_{a2} - X_{b4} \left( P_{rs1} - i \omega \Delta_N \right) \right) \right) \end{aligned} \right)}{\left( \begin{aligned} & \left( - \left( P_{is3} X_{b3} - P_{ip3} X_{b4} \right) \left( - X_{b4} Y_{a2} + X_{a2} Y_{b4} \right) + \left( X_{b4} Y_{b3} - X_{b3} Y_{b4} \right) \left( P_{rs3} X_{a2} - X_{b4} \left( P_{rs3} - i \omega \Delta_N \right) \right) \right) \\ & \left( - \left( P_{is1} X_{b3} - P_{ip1} X_{b4} \right) \left( - X_{b4} Y_{a1} + X_{a1} Y_{b4} \right) + \left( X_{b4} Y_{b3} - X_{b3} Y_{b4} \right) \left( P_{rs1} X_{a1} - X_{b4} \left( P_{rs1} - i \omega \Delta_N \right) \right) \right) \\ & + \left( - \left( P_{is3} X_{b3} - P_{ip3} X_{b4} \right) \left( - X_{b4} Y_{a1} + X_{a1} Y_{b4} \right) + \left( X_{b4} Y_{b3} - X_{b3} Y_{b4} \right) \left( P_{rs3} X_{a1} - X_{b4} \left( P_{rs3} - i \omega \Delta_N \right) \right) \right) \\ & \left( - \left( P_{is1} X_{b3} - P_{ip1} X_{b4} \right) \left( - X_{b4} Y_{a2} + X_{a2} Y_{b4} \right) + \left( X_{b4} Y_{b3} - X_{b3} Y_{b4} \right) \left( P_{rs1} X_{a2} - X_{b4} \left( P_{rs1} - i \omega \Delta_N \right) \right) \right) \end{aligned} \right)} \tag{14}$$

### 3. Model testing and actual work area application

#### (1) Model testing

In order to verify the feasibility of inverting the weakness of uncoupled interface fractures using the ANNI method, data from a fractured reservoir work area were selected to extract single-channel

seismic data for single-channel testing. A 30 Hz Ricker wavelet was used according to the central frequency of the actual work area seismic, the primary frequency was 30 Hz, the incident angle was assumed to be  $1^{\circ}\sim 30^{\circ}$ , and the initial stress was 20 MPa. In order to verify the stability, Gaussian random noise with signal-to-noise ratios of 2: 1 and 5: 1 was added, respectively. Fig. 3-1 shows the inversion results of the two fracture parameters under different signal-to-noise ratios.

In the inversion process, reasonable interpolation and extrapolation are performed in combination with the anisotropic parameters in the actual well, and the equivalent stiffness coefficient, slowness, polarization and fracture parameters are calculated using the anisotropic parameters and velocity density. The fracture parameters are smoothed and used as a low-frequency model to constrain the inversion results. In the initial stage, the range of the fracture parameters to be inverted and the number of parameters to be inverted are input. ANNI randomly generates an initial model that meets the number of parameters to be inverted within the range according to the range of parameters to be inverted and the number of parameters to be inverted, and then continuously cyclically corrects and finally obtains the inversion result. In the figure, the red dotted line represents the inversion result, the blue curve represents the actual data, and the black curve represents the input low-frequency model.

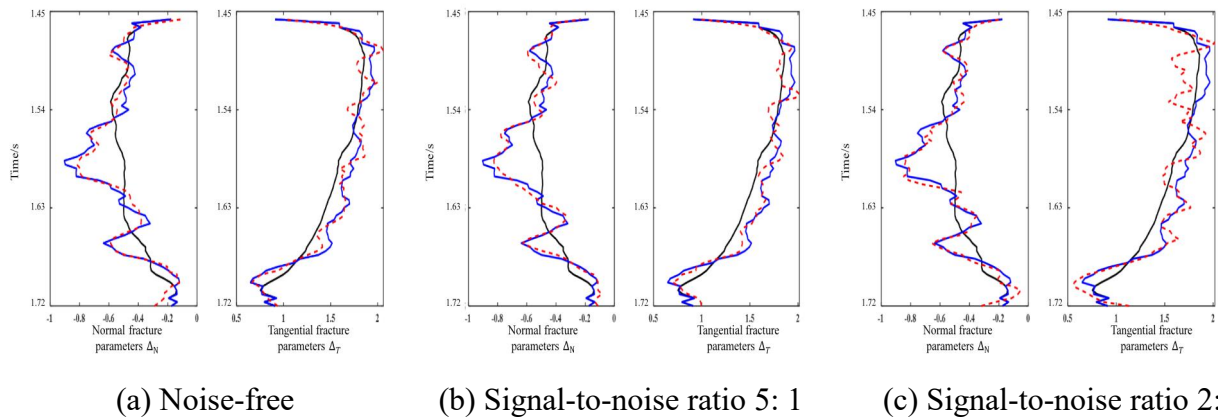
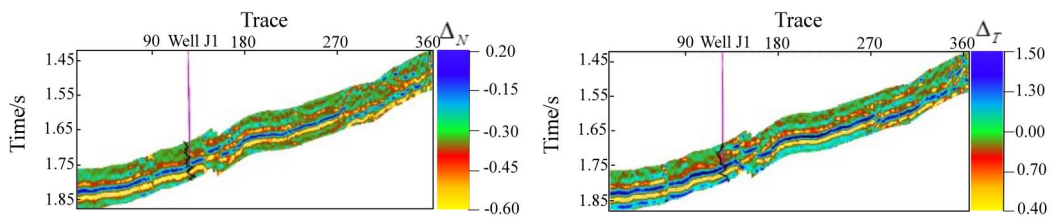


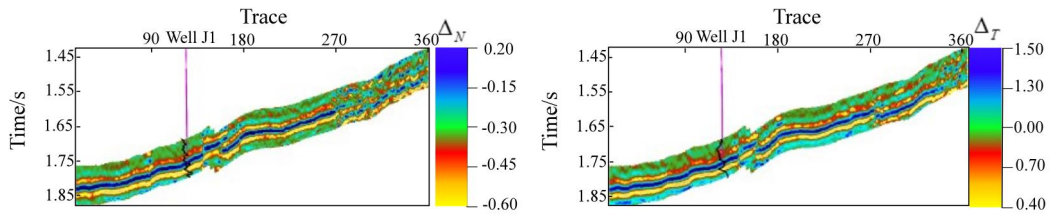
Fig. 3-1 Model inversion results with different signal-to-noise ratios

## (2) Application in actual work areas

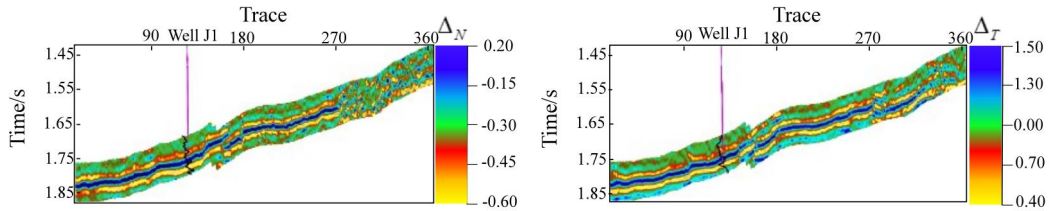
In order to verify the feasibility of the accurate equation inversion method in the actual work area, a fractured shale reservoir work area was selected. According to the well logging data, the well interpolation was reasonably extrapolated to obtain the Thomsen anisotropy parameters of the OA medium in the work area. The slowness, polarization, and other parameters required to solve the equation at different incident angles and azimuths can be obtained on this basis. The parameters that are independent of the parameters to be inverted are used. We are using the sub-waves extracted from the work area and combining the work area information, assuming that the frequency is 30 Hz and the incident angles are  $10^{\circ}$ ,  $20^{\circ}$ , and  $30^{\circ}$ . Fig. 3-2 shows the inversion profiles of the two fracture parameters, where the black curve is the well curve.



(a) Incident angle  $10^{\circ}$ ,  $\Delta_N$  inversion profile (b) Incident angle  $10^{\circ}$ ,  $\Delta_T$  inversion profile



(c) Incident angle  $20^\circ$ ,  $\Delta_N$  inversion profile (d) Incident angle  $20^\circ$ ,  $\Delta_T$  inversion profile



(e) Incident angle  $30^\circ$ ,  $\Delta_N$  inversion profile (f) Incident angle  $30^\circ$ ,  $\Delta_T$  inversion profile

Fig. 3-2 Results of profile inversion

It can be seen from the inversion results that the inverted interface parameters have a strong reflection in the target area near the well, which is consistent with the understanding of the work area here. In contrast, outside the target area, there are relatively scattered and chaotic reflections, which verifies the rationality of the method.

#### 4. Summary

Aiming at the inversion problem of OA medium under initial stress, the particular boundary conditions of the exact equation are used to construct the exact reflection coefficient equation and simplify the parameters irrelevant to the inversion, which further enriches the parameter types of pre-stack seismic inversion and contributes to overcoming the problem of insufficient consideration of interface parameter prediction. It can be seen from the inversion results of the model that the inversion results are in good agreement with the fracture parameters obtained by logging. Among them, the effect of the normal fracture parameters is due to the tangential fracture parameters. The profile inversion results compare the target layer and the non-target layer. There is a pronounced interface parameter response near the target well, and it is scattered reflection in the non-target layer. Through model testing and actual data application, the feasibility of this method in predicting fracture and stress parameters has been verified. However, due to the strong nonlinearity of the inversion operator and the large number of parameters to be inverted in the equation, further study is needed to enhance the reliability and stability of shale reservoir parameter prediction.

#### Acknowledgements

The authors acknowledge the sponsorship of National Natural Science Foundation of China (42174139, 41974119, 42030103), The Marine Science and Technology Fund of Shandong Province Marine Science and Technology Pilot National Laboratory (Qingdao) (2021QNLM020001-6), and Science Foundation from Innovation and Technology Support Program for Young Scientists in Colleges of Shandong Province and Ministry of Science and Technology of China (2019RA2136).

## References

- [1] CHEN F, ZONG Z, JIANG M. Seismic reflectivity and transmissivity parametrization with the effect of normal in situ stress [J]. *Geophysical Journal International*, 2021, 226(3): 1599-614.
- [2] MULARGIA F. The evaluation of Murnaghan constants as a function of pressure [J]. *Lettere al Nuovo Cimento* (1971-1985), 1979, 26(15): 471-6.
- [3] TRAYLOR T K, BURNLEY P C, WHITAKER M. Initial Acoustoelastic Measurements in Olivine: Investigating the Effect of Stress on P - and S - Wave Velocities [J]. *Journal of Geophysical Research: Solid Earth*, 2021, 126(11): e2021JB022494.
- [4] SCHOENBERG M. Elastic wave behavior across linear slip interfaces [J]. *The Journal of the Acoustical Society of America*, 1980, 68(5): 1516-21.
- [5] SCHOENBERG M, SAYERS C M. Seismic anisotropy of fractured rock [J]. *Geophysics*, 1995, 60(1): 204-11.
- [6] AKI K, RICHARDS P G. *Quantitative seismology* [M]. USA: University Science Books, 2002.
- [7] SHUEY R. A simplification of the Zoeppritz equations [J]. *Geophysics*, 1985, 50(4): 609-14.
- [8] STOVAS A, URSIN B. Reflection and transmission responses of layered transversely isotropic viscoelastic media [J]. *Geophysical Prospecting*, 2003, 51(5): 447-77.
- [9] SKOPINTSEVA L, AYZENBERG M, LANDRØ M, et al. Long-offset AVO inversion of PP reflections from plane interfaces using effective reflection coefficients [J]. *Geophysics*, 2011, 76(6): C65-C79.
- [10] LU J, YANG Z, WANG Y, et al. Joint PP and PS AVA seismic inversion using exact Zoeppritz equations [J]. *Geophysics*, 2015, 80(5): R239-R50.
- [11] YIN X-Y, CHENG G-S, ZONG Z-Y. Non-linear AVO inversion based on a novel exact PP reflection coefficient [J]. *Journal of Applied Geophysics*, 2018, 159: 408-17.
- [12] ZHANG F-Q, WEI F-J, WANG Y-C, et al. Generalized linear AVO inversion with the priori constraint of trivariate cauchy distribution based on Zoeppritz equation [J]. *Chinese Journal of Geophysics*, 2013, 56(6): 2098-115.
- [13] ZHOU L, LI J-Y, XH C, et al. Nonlinear three-term AVO inversion based on exact Zoeppritz equations; proceedings of the 78th EAGE Conference and Exhibition 2016, Vienna, F, 2016 [C]. European Association of Geoscientists & Engineers.
- [14] LANG K, YIN X, ZONG Z, et al. Anisotropic non-linear inversion based on a novel PP wave reflection coefficient for VTI media [J]. *IEEE Transactions on Geoscience and Remote Sensing*, 2023, 61.
- [15] MASON W P. *Physical acoustics: principles and methods* [M]. USA: Academic press, 2013.